Macromolecules

COMMUNICATION TO THE EDITOR

pubs.acs.org/Macromolecules

Subsurface Mapping of Amorphous Surface Layers on Poly(3-hexylthiophene)

M. Zerson,*[,†] E.-C. Spitzner,[†] C. Riesch,[†] R. Lohwasser,[‡] M. Thelakkat,[‡] and R. Magerle*[,†]

[†]Fakultät für Naturwissenschaften, Technische Universität Chemnitz, Chemnitz, Germany

[‡]Angewandte Funktionspolymere, Makromolekulare Chemie I, Universität Bayreuth, Bayreuth, Germany

Conjugated polymers like poly(3-hexylthiophene) (P3HT) and other thiophene-based polymers are promising materials for polymeric electronic devices and are considered as prototype semiconducting polymers for fundamental studies.[1] P3HT exhibits excellent electronic properties, in particular, high charge-carrier mobility. This is attributed to the intermolecular $\pi-\pi$ stacking of the conjugated backbones, causing delocalization of the electronic states within the crystalline regions of semicrystalline P3HT.[2,3] The correlation between the electronic properties and the complex hierarchical microstructure of semicrystalline polymers for organic electronic devices, including P3HT, is currently of great interest. P3HT forms lamellar crystals that are embedded in an amorphous matrix. The detailed microstructure and crystallinity depend on the stereoregularity of the polymer backbone, the molecular weight, the structure of the side chains, and the details of the film processing conditions.[4−6] In general, a large degree of order within the crystalline regions is considered to be essential for a high charge-carrier mobility.[2,3] Processing and annealing conditions can either improve or deteriorate the electrical properties of P3HT. Additionally, when cast from solution, crystalline P3HT fibers can be formed and deposited on the surface.[7,8] The nanoscale morphology of P3HT is frequently inferred from atomic force microscopy (AFM) images of the surface of thin films and is related to changes in the material's electronic properties, which may affect an organic electronic device's performance. The detailed surface structure is also of particular importance for the charge-transfer process between the polymeric material and the electrodes. Up to now, studies have addressed the morphology of crystalline regions at the surface of polythiophene films.[2,4] However, little attention has been paid to the distribution of the amorphous components at the surface of polythiophene films. Sakai et al. have reported a 3 nm thick amorphous layer on crystalline regions of polypropylene, a common semicrystalline polymer.[9] With depth-resolved AFM imaging, we have recently shown that the edges of crystalline lamella in polypropylenes with a low degree of crystallinity are covered by an ∼10 nm thick amorphous layer.[10−12]

In this Communication, we use this method for extending our study on the surface structure of a well-defined, regioregular type of P3HT with depth-resolved AFM. In particular, we determine the local thickness of compliant surface layers by measuring the small but finite indentation of the AFM tip into the surface. We discovered that the entire surface of highly crystalline thin films of a well-defined, regioregular type of P3HT is covered by an amorphous layer of P3HT. On the as-cast film, the amorphous layer is 7 nm thick. After annealing at 230 °C, it decreases to 5 nm. The presence of the amorphous surface layer can have important consequences on the electronic properties of P3HT surfaces and the performance of thin-film electronic devices using P3HT.

We study a highly regioregular type of P3HT with a well-defined molecular weight M_n = 10.2 kg/mol (measured with size-exclusion chromatography) and a low polydispersity index 1.19 synthesized by Grignard metathesis polymerization as described previously.[4,13] The hierarchical-structure-formation process of polymer crystallization and side-chain ordering has been studied for P3HT of this molecular weight with X-ray diffraction and differential scanning calorimetry.[4] Here, about 100 nm thick films were prepared by spin-casting a 1 wt % solution of P3HT in chloroform onto polished Si wafers covered with a native oxide layer. One film was annealed above the melting temperature T_m = 227 °C of this particular P3HT. Annealing took place at 230 °C for 20 min in an Ar atmosphere followed by slow cooling (within ∼30 min) to room temperature. The detailed AFM data acquisition and analysis protocols are described in ref 12. Briefly, for constructing a depth profile, the amplitude A and the phase φ of the oscillating cantilever are recorded as a function of the tip−sample distance. From this amplitude−phase−distance (APD) data, the position of the true surface, h_0, and the tip indentation $\tilde{z}$ into the compliant film are determined.[14] The tip indentation $\tilde{z}$ is used as a depth coordinate relative to the true surface h_0 for the construction of the depth profiles of k_{TS}, the conservative contribution to the tip−sample interaction,[15] and E_{dis}. The latter is the energy dissipated between the tip and the sample during one tip oscillation cycle, which is a measure of the dissipative part of the tip−sample interaction.[16]

Figure 1 shows conventional AFM height and phase images of an as-cast P3HT film. The displayed area was chosen to show the characteristic features frequently found in AFM images of P3HT.[2,4,5] The two 30 nm wide, crystalline P3HT fibers oriented diagonally across the imaged area are ∼10 nm high. Such fibers are known to form in solution[7,8] and are deposited on the film surface during spin-casting. Furthermore, a fine texture of ∼10 nm wide bright stripes is visible in the phase image (Figure 1b). These stripes correspond to the lamellar crystalline regions within the semicrystalline P3HT. The isolated 70 nm large round dark area visible in the phase image corresponds to a 10 nm deep depression in the conventional AFM height image. APD data were measured at 75 × 22 points within the area marked by the white rectangle. The shape of the true surface reconstructed from the APD data

Received: May 17, 2011
Revised: June 23, 2011
Published: July 08, 2011

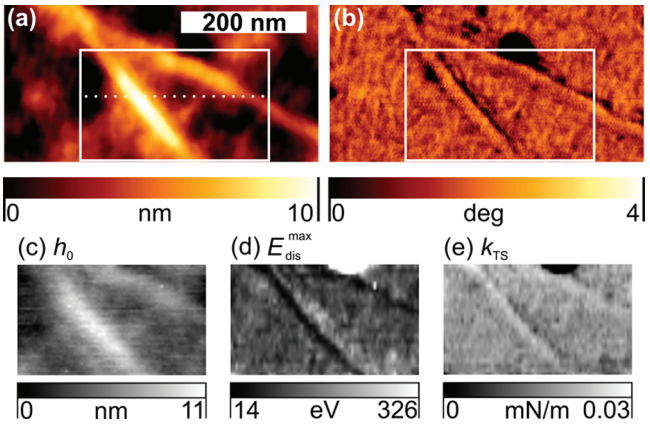

Figure 1. (a, b) AM-AFM height and phase images of an as-cast P3HT film. Bright (dark) areas in (b) correspond to the crystalline (amorphous) regions. The white rectangle indicates the area where the APD data were measured. Corresponding maps reconstructed from the APD data: (c) true surface h_0, (d) maximum dissipated energy E_{dis}^{max}, and (e) k_{TS} computed for an amplitude ratio of $A/A_0 = 0.9$. The dotted line marks the position of the depth profiles shown in Figure 3.

(Figure 1c) shows fewer corrugations than the conventional AFM height image (Figure 1a). Also, the two fibers have a broader shape. The difference between the shape of the true surface and the conventional AFM height image is due to the indentation of the AFM tip into the compliant surface layer. For both methods, the tip indentation depends on the amplitude ratio A/A_0. From maps of APD data, maps of the tip indentation can be determined (not shown here) which reflect local differences in the compliance of the material. Furthermore, these maps of local material properties can elucidate quantities such as the conservative contribution to the tip−sample interaction, k_{TS} (Figure 1e), and the maximal energy E_{dis}^{max} dissipated between the tip and the sample at each pixel (Figure 1d). In the E_{dis}^{max} map, the fibers appear dark, corresponding to less dissipated energy and a lower loss modulus than the surrounding material. In the k_{TS} map, the P3HT fibers appear as bright stripes, indicating that they are stiffer than the surrounding material. The maps of k_{TS} and E_{dis}^{max} validate the interpretation of the conventional AFM phase image (Figure 1b). The 70 nm large round dark area in the upper half of the AFM phase image has significantly lower k_{TS} and higher E_{dis}^{max} values than its surroundings. Furthermore, no depression is observed at this spot in the true surface map. We therefore consider this area to represent a domain of a soft (compliant) material that is segregated at the surface.

While annealing the sample above its melting temperature, all crystals melt, and during the cooling process, the material crystallizes again. The resulting surface structure (Figure 2) resembles the lamellar structure previously observed for P3HT with this molecular weight.[4] Conventional AFM height images of a larger area (not shown here) show an increase in the roughness as well as a nanoscale texture similar to that of the corresponding phase images (Figure 2b). The latter shows well-differentiated regions of bright stripes that are aligned parallel locally. These bright stripes correspond to the characteristic crystalline lamellae. Another feature frequently observed in conventional AFM phase images of P3HT is 20−50 nm wide dark domains, marked by D in Figure 2b, which are similar to those on the as-cast film. After annealing, these domains are smaller and less frequent than before annealing.

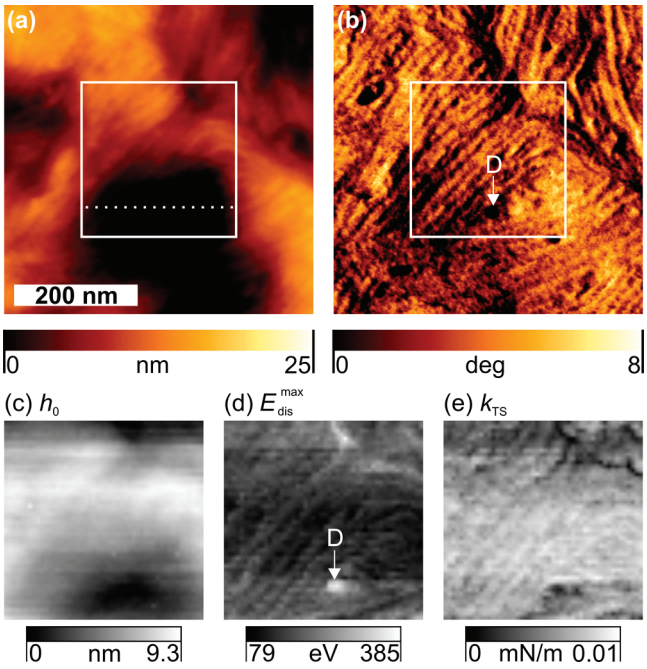

Figure 2. Same as Figure 1 for a P3HT film annealed at 230 °C for 20 min. In (d), an ∼30 nm large domain with high values of E_{dis}^{max} is marked by the letter D.

APD data were measured at 50 × 50 points within the area indicated (as white square) in Figure 2a,b. The true surface reconstructed from the APD data has the same shape as the AFM height image, however, without the fine nanoscale texture. The map of the maximal energy E_{dis}^{max} dissipated between the tip and the sample (Figure 2d) shows the same pattern as the conventional AFM phase image, however, with an inverted contrast. The dark stripes in the AFM phase image correspond to bright stripes in the E_{dis}^{max} map. These regions correspond to the soft, amorphous regions between the crystalline lamella. In the k_{TS} map, they appear as bright stripes (Figure 2e). The round, dark spots in the AFM phase image (marked by D) correspond to bright dots in the E_{dis}^{max} map and dark dots in the k_{TS} map. We therefore attribute these dots to the domains of a soft (compliant) material that is segregated at the surface. The interpretation of the AFM phase image, the E_{dis}^{max} map, and the k_{TS} map is in accordance with previous results on semicrystalline polypropylene as well as block copolymers forming hard domains within a soft matrix.[12,14]

From the maps of the APD data, we determined the dissipated energy E_{dis} and the conservative contribution to the tip−sample interaction k_{TS} as a function of the indentation depth $\tilde{z}$. The depth profiles of k_{TS} and E_{dis} are shown in Figure 3 for the as-cast and the annealed P3HT film. The depth profiles have been reconstructed at the positions marked with dashed lines in the height images in Figures 1a and 2a. The enlarged details of the AFM phase images at the position of the cross sections are shown in Figures 3c and 3f, respectively. The conservative contribution to the tip−sample interaction k_{TS} increases with indentation depth $\tilde{z}$ and reaches its highest value at the greatest value of the indentation depth (Figure 3a). Larger depths cannot be probed with this technique. The maximum indentation depth can be directly inferred from the depth profiles. It is a measure of the local thickness of a compliant layer that is covering the surface. On the as-cast film, the mean thickness of this compliant layer is 7 nm

dx.doi.org/10.1021/ma2011359 |*Macromolecules* 2011, 44, 5874–5877

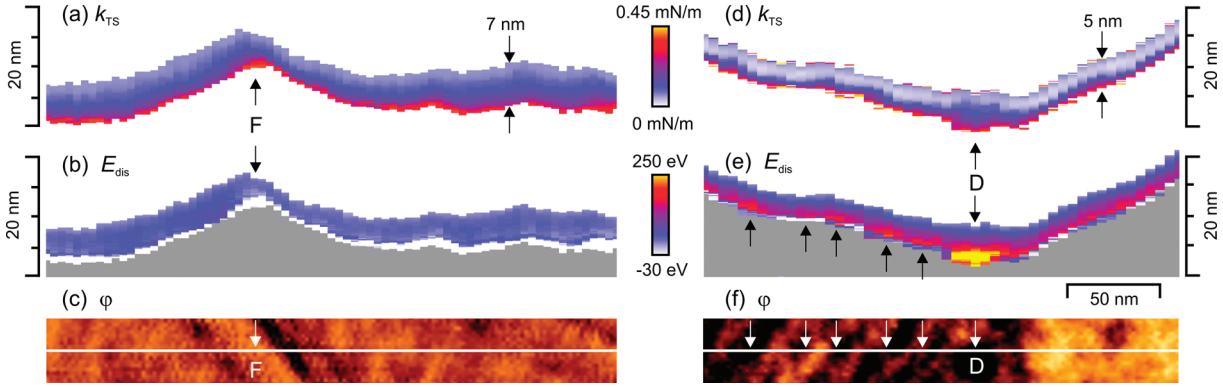

Figure 3. (a, b) Depth profiles of k_{TS} and E_{dis} for an as-cast P3HT film at the position indicated in the AFM phase image shown in (c) and in the height image in Figure 1a. The gray area corresponds to depths larger than the largest tip indentation. (d, e) Depth profiles of k_{TS} and E_{dis} for the P3HT film annealed at 230 °C for 20 min measured at the position indicated in the phase image shown in (f) and in the height image in Figure 2a. The arrows mark the local maxima of E_{dis}, which correspond to the amorphous regions between the crystalline lamellae. On the as-cast film, the laterally averaged thickness of the amorphous top layer is 7 nm. After annealing at 230 °C, the amorphous layer is on average 5 nm thick.

with a standard deviation of 1 nm. After annealing at 230 °C, the laterally averaged thickness of this compliant layer is reduced to 5 ± 1 nm. We identify this soft surface layer as the amorphous fraction of the semicrystalline P3HT. Because of the high purity of the P3HT used for this study, the possibility that this soft layer originates from any impurities segregating at the surface can be excluded. Our data show that the entire surface and, in particular, the crystalline lamellae and the crystalline fibers are covered by this amorphous layer of P3HT. The shape of the true surface shows no regular structure (texture) that is reminiscent of the average distance of the crystalline lamellae. On this length scale (<100 nm), the true surface is flat. The glass transition temperature of the type of P3HT studied is −10 °C;[4] therefore, at room temperature, the amorphous P3HT is a highly viscous fluid and the surface tension causes the formation of a smooth surface. Two factors could contribute to an accumulation of amorphous P3HT at the film surface. First, less crystallizable material is rejected from the growth front as the lamellae grow toward the surface. Second, if the surface tension of amorphous P3HT is lower than that of crystalline P3HT, this could inhibit the crystal growth front from reaching the surface. The reduction in the thickness of the amorphous layer after annealing is most likely caused by the further growth of crystalline lamellae toward the film surface, which accompanies the growth of lamellae within the film plane. The presence of an amorphous surface layer is in accordance with earlier findings on the surface properties of semicrystalline polypropylene.[9,11,12]

In summary, we have demonstrated depth-resolved mapping of the subsurface structure of a semiconducting semicrystalline polymer. Our data show that the entire surface of a highly regioregular P3HT, including crystalline regions and crystalline fibers, is covered by an amorphous layer. On the as-cast film, it is on average 7 nm thick. After annealing at 230 °C, its thickness decreases to 5 nm. The presence of the amorphous surface layer can have important consequences. For instance, it can influence the charge-transfer process between P3HT and electron acceptor materials as well as the charge extraction at the electrodes. It might also influence the alignment of electronic levels at these interfaces. Since annealing causes changes within the amorphous surface layer, possible contributions of amorphous surface layers toward electronic properties and/or device performance should be considered.

AUTHOR INFORMATION

Corresponding Author

*E-mail: mario.zerson@physik.tu-chemnitz.de (M.Z.); robert.magerle@physik.tu-chemnitz.de (R.M.).

ACKNOWLEDGMENT

This work has been supported by the Deutsche Forschungsgemeinschaft (SPP 1355) and the Volkswagen Foundation.

REFERENCES

(1) Perepichka, I. F., Perepichka, D. F., Eds. *Handbook of Thiophene-Based Materials: Applications in Organic Electronics and Photonics*; John Wiley & Sons, Ltd.: Chichester, UK, 2009.

(2) Kline, R. J.; McGehee, M. D.; Kadnikova, E. N.; Liu, J.; Fréchet, J. M. J.; Toney, M. F. *Macromolecules* **2005**, *38*, 3312–3319.

(3) Sirringhaus, H.; Brown, P. J.; Friend, R. H.; Nielsen, M. M.; Bechgaard, K.; Langeveld-Voss, B. M. W.; Spiering, A. J. H.; Janssen, R. A. J.; Meijer, E. W.; Herwig, P.; de Leeuw, D. M. *Nature* **1999**, *401*, 685–688.

(4) Wu, Z.; Petzold, A.; Henze, T.; Thurn-Albrecht, T.; Lohwasser, R. H.; Sommer, M.; Thelakkat, M. *Macromolecules* **2010**, *43*, 4646–4653.

(5) Hugger, S.; Thomann, R.; Heinzel, T.; Thurn-Albrecht, T. *Colloid Polym. Sci.* **2004**, *282*, 932–938.

(6) Gang, L.; Vishal, S.; Yan, Y.; Yang, Y. *J. Appl. Phys.* **2005**, *98*, 043704.

(7) Oosterbaan, W. D.; Vrindts, V.; Berson, S.; Guillerez, S.; Douheret, O.; Ruttens, B.; D'Haen, J.; Adriaensens, P.; Manca, J.; Lutsen, L.; Vanderzande, D. *J. Mater. Chem.* **2009**, *19*, 5424–5435.

(8) Ihn, K. J.; Moulton, J.; Smith, P. *J. Polym. Sci., Part B: Polym. Phys.* **1993**, *31*, 735–742.

(9) Sakai, A.; Tanaka, K.; Fujii, Y.; Nagamura, T.; Kajiyama, T. *Polymer* **2005**, *46*, 429–437.

(10) Dietz, C.; Zerson, M.; Riesch, C.; Gigler, A. M.; Stark, R. W.; Rehse, N.; Magerle, R. *Appl. Phys. Lett.* **2008**, *92*, 143107.

(11) Dietz, C.; Zerson, M.; Riesch, C.; Franke, M.; Magerle, R. *Macromolecules* **2008**, *41*, 9259–9266.

(12) Spitzner, E.-C.; Riesch, C.; Magerle, R. *ACS Nano* **2011**, *5*, 315–320.

(13) Sheina, E. E.; Liu, J.; Iovu, M. C.; Laird, D. W.; McCullough, R. D. *Macromolecules* **2004**, *37*, 3526–3528.

(14) Knoll, A.; Magerle, R.; Krausch, G. *Macromolecules* **2001**, *34*, 4159–4165.
(15) Schröter, K.; Petzold, A.; Henze, T.; Thurn-Albrecht, T. *Macromolecules* **2009**, *42*, 1114–1124.
(16) García, R.; Gómez, C. J.; Martinez, N. F.; Patil, S.; Dietz, C.; Magerle, R. *Phys. Rev. Lett.* **2006**, *97*, 016103.